JOURNAL OF CATALYSIS 102, 10–20 (1986)

# The Structure of Coprecipitated Aluminophosphate Catalyst Supports

T. T. P. CHEUNG, K. W. WILLCOX, M. P. MCDANIEL, AND M. M. JOHNSON

*Phillips Research Center, Bartlesville, Oklahoma 74004*

AND

C. BRONNIMANN AND J. FRYE

*Colorado State University, Fort Collins, Colorado 80523*

Received January 14, 1986; revised May 11, 1986

Porous aluminophosphates, which are useful as catalyst supports for polymerization, isomerization, or other hydrocarbon conversions, can be made by coprecipitation when an acidic solution of $Al^{3+}$ and $PO_4^{3-}$ ions is neutralized. When the P/Al ratio in solution is equal to or greater than one, $AlPO_4$ is obtained often as a crystalline material, leaving the excess phosphate in solution. However, when excess $Al^{3+}$ is present in solution (P/Al < 1) then it also precipitates and the resulting support retains a similar P/Al ratio to that in solution. In this study the structure of such aluminophosphates has been examined by means of X-ray diffraction and high resolution solid state NMR spectroscopy using both $^{27}Al$ and $^{31}P$ nuclei. These materials are not simple coprecipitated mixtures of $Al_2O_3$ and $AlPO_4$. In fact, no evidence for the presence of either species was detected. Instead they appear to be amorphous structures in which the phosphate is randomly dispersed, and the aluminum exists in one octahedral and several different tetrahedral environments. Results from ethylene polymerization over these catalysts also support this view.

## INTRODUCTION

Aluminum phosphate has long been known as a catalyst support (*1, 2*). Its close relationship to silica, which is isoelectronic and isostructural, has made it an interesting carrier for numerous catalytic applications (*2*). But unlike silica, it also has an acidic character due to surface phosphate (*4–6*). This gives it a potent isomerization activity of its own. Like silica, $AlPO_4$ has many structural forms, all fairly well characterized (*3*).

$AlPO_4$ is usually prepared by neutralizing an acidic solution of $Al^{3+}$ and $PO_4^{3-}$ ions. If the precipitation occurs from a solution having less than the stoichiometric amount of phosphate, the precipitate sometimes reflects this composition. These materials, having a P/Al ratio less than unity, are known as aluminophosphates and are much less well characterized than pure alumina or aluminum phosphate (*7*). Their utility as polymerization catalyst supports has recently generated some commerical interest (*8–10*).

Although sometimes described as $AlPO_4$–$Al_2O_3$ composites, Hill *et al.* (*11*) have noted that the aluminophosphates show none of the characteristics of alumina, either in photomicrographs or in the X-ray diffraction patterns. Other workers have observed differences in surface area, heat stability, and other catalytic properties between $AlPO_4$ and the aluminophosphates (*4, 11–17*). Recently Vogel and Marcelin (*13*) have reported that even when precipitating from a stoichiometric solution (P/Al = 1.0), dramatic variations in composition and properties can be obtained at different gelation conditions. In particular they note that at the higher pH values (pH 6, where



0021-9517/86 $3.00

the most interesting supports are often made) excess aluminum may have a tendency to precipitate with the phosphate.

In this report we have attempted to further examine the structure of these aluminophosphate supports. In particular, we were interested to know whether these materials were composites of "free" alumina and aluminum phosphate, or whether the precipitation resulted in a truly random arrangement. Besides the usual technique of X-ray diffraction (XRD), which describes long range order, we have also enlisted the aid of solid state $^{27}Al$ and $^{31}P$ NMR to describe the local environment around these nuclei. Previous workers have successfully used $^{27}Al$ NMR to distinguish between different types of Al–O coordination, such as $AlO_4$ tetrahedral versus $AlO_6$ octahedral, in alumina (*18, 19*) and other aluminum–oxygen compounds (*20–22*). Other have applied $^{31}P$ NMR to study acid sites in zeolites (*23*). In our study this information has then been coupled with ethylene polymerization studies over the catalyst to arrive at a uniform picture of the system.

## EXPERIMENTAL

*Catalyst preparation.* Aluminophosphate samples were prepared by adding ammonium hydroxide to concentrated acidic solutions of aluminum nitrate and ammonium phosphate. Precipitation was done rapidly and from concentrated solution. After neutralization with ammonium hydroxide to pH 6–7, the precipitate was aged in dilute ammonia water at pH 8 for 1 h at 80°C, then washed several times with water, and finally alcohol. Then it was dried in a vacuum oven at 100°C overnight.

This preparation was a little different from that usually employed by previous workers: during precipitation the pH was not held constant. As ammonia was added to the aluminum- and phosphate-containing solution, the pH rose from less than one to neutrality, and precipitation occurred during the interval. It is possible, although not certain, that this could lead to less homogeneity in the precipitate than adding both solutions simultaneously to a third vessel of fixed pH. It was nevertheless chosen because it seems to produce a more active catalyst material, by our tests at least. The precipitation did occur very rapidly—the ammonia solution was added in less than 30 s—which probably favors homogeneity. The final aging step at pH 8 tends to increase porosity and decrease surface area.

For polymerization studies, these samples were then impregnated with a solution of chromium acetate to equal 0.2 mmole/g. After being dried again samples were activated by fluidization in dry air at 0.15 ft/s to 600°C where they were held for 3 h. The heating rate was 400°C/h. This treatment leaves most of the chromium as a hexavalent surface species (*10*). The activated samples were then stored under dry nitrogen until needed.

The composition of the final catalyst, that is, the P/Al ratio, was determined by X-ray fluorescence on the calcined sample. We found that calcining did not change the composition. Porosity measurements were taken by mercury porosimetry, and surface areas by the usual BET method.

*NMR instrumentation.* A typical problem encountered in obtaining high resolution $^{27}Al$ NMR spectra in solids is that $^{27}Al$ (wih a nuclear spin of 5/2) suffers considerable quadrupolar broadening. While in principle magic angle spinning (MAS) can narrow such a broadening considerably, the typical 4 to 6 kHz spinning speed achieved by most commercial spectrometers is inadequate because spinning sidebands remain near the central part of the spectrum, distorting the spectrum. Fortunately the $^{27}Al$ NMR experiments described below have utilized the extremely high speed rotor developed by G. E. Maciel's group, which can develop speeds exceeding 11 kHz. With such a spinning rate, the interference from spinning sidebands can be eliminated completely.

The NMR measurements were carried out at the Colorado State University re-

gional NMR Center. All spectra were obtained with conventional Fourier transform technique in combination with MAS. $^{27}Al$ NMR spectra were obtained from a modified Nicolet NT-360 spectrometer with $^{27}Al$ frequency at 93.8 MHz and a sample spinning rate of at least 11 kHz. The $^{31}P$ spectra were collected from a modified Nicolet NT-150 spectrometer at a frequency of 60.7 MHz for $^{31}P$ and a spinning speed between 3.5 and 4 kHz. The $^{27}Al$ NMR chemical shifts are referred to external $KAl(SO_4)_2 \cdot 12H_2O$ which has a chemical shift of 1.1 ppm from $AlCl_3 \cdot 6H_2O$. The $^{31}P$ NMR chemical shifts are referred to external $H_3PO_4$ (85%). Dry nitrogen was used to drive the MAS rotor.

All NMR samples were calcined in dry air for 3 h at 600°C, then stored under dry nitrogen. Loading into sample rotors was done in a moisture-free glove box. the aluminophosphates were prepared as described above. At P/Al = 0 a commerical Ketjen grade B $\gamma$-alumina was also used as a reference.

*Ethylene polymerization.* Runs were conducted at 95°C in a stirred 2-liter jacketed autoclave. Typically about 40 mg of catalyst was charged under nitrogen, then 1-liter of isobutane liquid was added as diluent, and finally ethylene was supplied on demand at 550 psig for 30 min. Polymerization rates were determined by monitoring the flow of ethylene into the reactor through a mass flowmeter. At the end of the run the isobutane was flashed off, leaving about 100–200 g of dry polyethylene. The isobutane also contained 8 ppm of triethylborane as scavenger. The reactor jacket contained boiling alcohol under controlled pressure in order to maintain reactor temperature within 0.5°C.

*Other instrumentation.* Thermogravimetric analysis (TGA) of samples was done on a DuPont 950 Thermogravimetric Analyzer connected to a 1090 Thermal Analyzer. Samples with a typical weight of 10 mg were heated at 10°C/min in a stream of dry nitrogen. X-Ray diffraction patterns were obtained in reflection mode on a Philips Electronics X-ray diffractometer using a copper target.

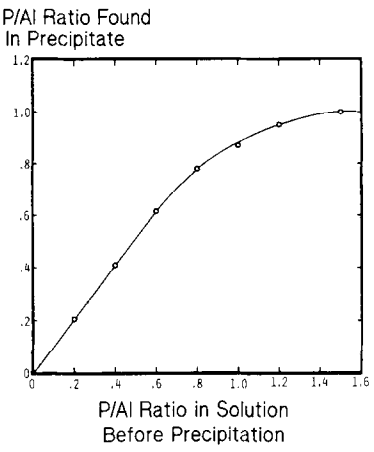


FIG. 1. The composition of the precipitate depends on the composition of the solution before precipitation, but the two are not always equal.

## RESULTS AND DISCUSSION

### *Precipitate Composition*

Figure 1 shows how the composition of the solution before precipitation affects the composition of the precipitate. Below P/Al = 0.8 there is no difference between the two, within experimental error. The precipitate contains exactly the same relative amounts of aluminum and phosphate as existed in solution before precipitation. Above P/Al = 0.8, however, precipitation of phosphate becomes less efficient by this method. The precipitate P/Al ratio approaches unity but never exceeds it, even when there is 50% excess phosphate in solution.

### *Porosity*

Since precipitation was conducted rapidly in this study from concentrated solutions, all of these supports were found to be highly porous. One indication is the surface area after calcination at 600°C, which is shown in Fig. 2. A large rise in surface area, about 100 $m^2/g$, is seen between P/Al = 0 and P/Al = 0.2, indicating that even this

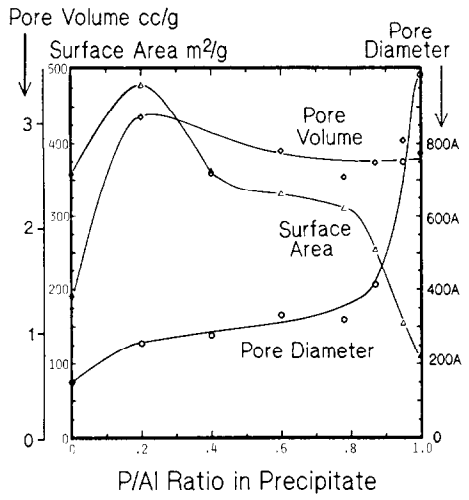


FIG. 2. Porosity of aluminophosphates calcined at 600°C, as a function of P/Al ratio in the precipitate. Pore volume was determined by mercury intrusion into pores smaller than $10^4$ Å. The average pore diameter was calculated from 4(pore vol)/(surface area).

first addition of phosphate has a profound effect on the structure of the precipitate. This rise was seen by us on more than one occasion, and is also visible in data of Schmidtmeyer and Moffat (*14*) and Kearby (*16*). Beyond P/Al = 0.2 area declines gradually with further addition of phosphate, and drops off steeply as P/Al approaches unity, suggesting a second transition.

This general trend has also been reported by Marcelin *et al.* (*12*) and by Schmidtmeyer and Moffat (*14*), both of whom employed a slightly different preparation method than that used here. They slowly added two solution—one containing aluminum and phosphate ions, the other diluted ammonia water—to a third vessel containing water, so that the precipitation occurred in a dilute medium at a constant pH. In contrast we used very concentrated solutions, and rapidly added ammonia to the salts, so the pH increased during the precipitation. This difference in preparation does seem to have resulted in higher surface areas.

A similar behavior can be seen in the pore volume of these materials, which was determined by mercury intrusion into samples calcined at 600°C. The total penetration (5 $\mu$m down to 30 Å) is plotted in Fig. 2. Again there is a very obvious change in structure with the first addition of phosphate, because pore volume increases dramatically between P/Al = 0 and 0.2. At higher phosphate levels the pore volume remains fairly constant.

An analysis of this pore volume is shown in Fig. 3. Notice that at P/Al = 0 almost all of the porosity is in small pores, those having a diameter less than 100 Å. By P/Al = 0.2, however, there is a significant decrease in small pores and a tremendous rise in mid-size and larger pores, those greater than 100 Å. Then with further additions of phosphate, there is a gradual shift toward larger pores. As P/Al approaches unity the shift becomes very pronounced, signaling another transition. These two transitions are especially evident in the average pore diameter which is plotted in Fig. 2. Marcelin *et al.* also report that pore diameter increases with P/Al ratio for samples precipitated at constant pH (*12*).

At other calcining temperatures the sur-

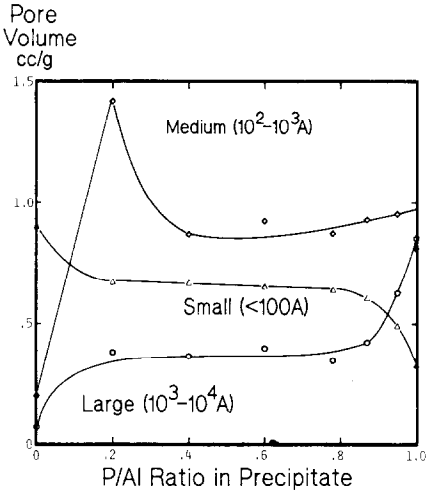


FIG. 3. Pore volume distribution of aluminophosphates calcined at 600°C as a function of P/Al ratio. Most of the volume is inside mid-size pores (diameter $10^2$–$10^3$ Å), where there is a dramatic change with the first addition of phosphate.

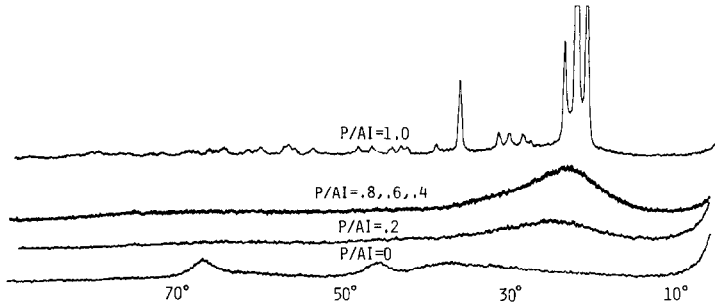


FIG. 4. X-Ray diffraction patterns of aluminophosphates after being calcined at 600°C.

face area profile was similar to that at 600°C in Fig. 2. In general the presence of phosphate seems to help the thermal stability of the structure. This is shown in Table 1, which lists the percent of surface lost between 200 and 800°C for each sample. Notice that the largest effect comes again between P/Al = 0 and 0.2, and approaching P/Al = 1.0.

*X-Ray Diffraction*

XRD powder patterns of these samples were similar to those reported by previous workers for other preparations. They are shown in Fig. 4, where each sample was calcined at 600°C. As expected, precipitation in the absence of phosphate under our conditions yielded boehmite after the sample was dried at 100°C, and this changed to $\gamma$-alumina after calcination. The broad XRD pattern indicates a low order of crystallinity.

The first addition of phosphate changes the spectrum, giving no XRD pattern at all for the 100°C 0.2 P/Al sample. By 400°C a new peak at $2\theta = 24°$ emerges, which is characteristic of the tetrahedral structure in amorphous silica or $AlPO_4$. This pattern remains unchanged at 700 or even 850°C.

Further additions of phosphate strengthen the peak at 24°. Samples containing P/Al = 0.4, 0.6, or 0.8 exhibit no hint of alumina or boehmite. At 100°C the XRD spectrum is again totally flat, but by 200°C the peak at 24° begins to emerge. Further calcining at higher temperatures sharpens this peak somewhat, but no new lines appear, even at 950°C.

When the phosphate level reaches P/Al = 1.0 the tridymite form of $AlPO_4$ becomes clear, even at 100°C. The degree of crystallinity does seem to vary with gelation conditions, as reported by Vogel and Marcelin (*13*). Under our precipitation conditions at pH 6–7, it took excess phosphate in solution to obtain the crystalline spectrum. In fact, when the solution contained exactly P/Al = 1.0, the precipitate level of phosphate was slightly less and the amorphous spectrum resulted. Calcining at higher temperatures, even to 950°C, did not promote crystallization.

*Thermogravimetric analysis*

The precipitates were also heated slowly in a TGA apparatus to 1000°C while the weight loss was monitored to detect the release of moisture. A few of these weight–

TABLE 1

| P/Al in precipitate | Surface area at 800°C | Percent loss from 200 to 800°C |
|---|---|---|
| 0 | 359 | 31 |
| 0.2 | 470 | 18 |
| 0.4 | 338 | 21 |
| 0.6 | 313 | 16 |
| 0.78 | 298 | 20 |
| 0.87 | 236 | 6 |
| 0.97 | 151 | 9 |
| 1.00 | 116 | 8 |

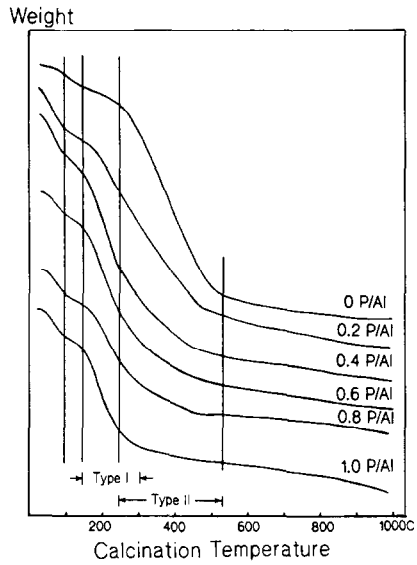


FIG. 5. Thermogravimetric analyses of various aluminophosphates. Four transition temperatures are marked on each curve—100, 150, 250, and 520°C.

temperature profiles are shown in Fig. 5. They are characterized by several transition points which can be seen in most of the samples.

As each sample was heated, starting at 25°C, the first point that becomes evident is at 100°C, which corresponds to the boiling off of water held loosely in the pores. The weight loss before 100°C is rapid due to the release of this water. After 100°C the water is gone, so the curve flattens out.

The second release of moisture is very large and clearly marked by several transition temperatures in all of the samples. It occurs between 150°C and about 550°C, depending on the P/Al ratio, and corresponds to the release of about 1 mole of water per mole of aluminum in the sample, regardless of the phosphate content. After 550°C each curve flattens out again and the gradual weight loss to 1000°C is probably due mainly to condensation of surface hydroxyls.

From a qualitative perspective we find once again that the first addition of phosphate has a dramatic effect on these profiles. At P/Al = 0 this release of 1 $H_2O$ per Al begins at 250°C, but at P/Al = 0.2 the release has shifted to 150°C, and remains there with further additions of phosphate.

Actually two types of water release seem to occur between 150°C and 550°C. They are apparent in the two extremes of Fig. 5, that is, at P/Al = 0 and 1.0. Type I release (P/Al = 1.0) begins at about 150°C and is over by say 300°C. Type II release (P/Al = 0) requires much higher temperatures, beginning at 250°C and ending at 500–550°C. At intermediate phosphate levels, combinations of the two types can be seen, and the fraction of moisture lost during the Type I transition roughly corresponds to the P/Al ratio (i.e., Type I/total = P/Al). For example, at P/Al = 0.4 two breaks in the curve can be seen in this temperature region, one at 150°C and another at 250°C. The loss is the range 150–250°C is about 40% of the total loss at 150–550°C. However, there is enough overlap between the two transitions that one cannot be quantitative.

### *$^{27}$Al Solid State NMR*

Results from $^{27}$Al NMR are shown in Fig. 6. The distinct advantage of employing high spinning speed (>11 kHz) can be clearly seen, because the spinning sidebands are at

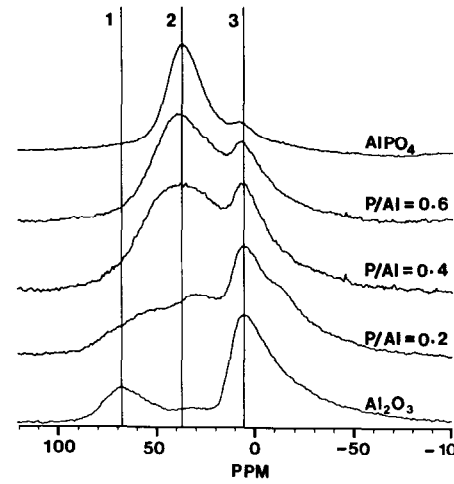


FIG. 6. 93.8-MHz $^{27}$Al solid state NMR spectra of $AlPO_4$, aluminophosphates and $\gamma$-$Al_2O_3$ with $KAl(SO_4)_2 \cdot 12H_2O$ as an external reference.

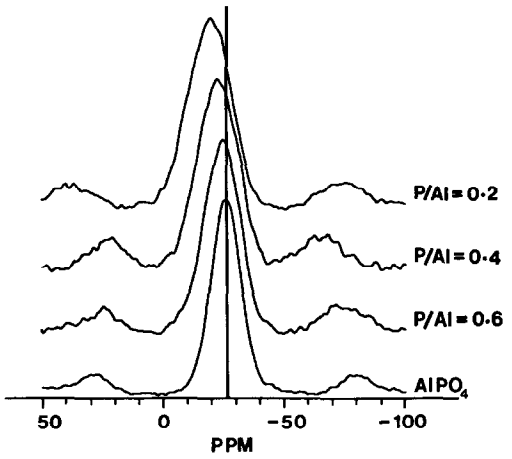


FIG. 7. 60.7 MHz $^{31}P$ solid-state NMR spectra of $AlPO_4$ and aluminophosphates with $H_3PO_4$ (85%) as an external reference.

least 100 ppm away from the main region of the spectra. Therefore spectral features are not distorted by these sidebands. In Fig. 6, the $\gamma$-$Al_2O_3$ sample shows two resonances, one at 66 ppm (labeled as peak 1 in the figure) and the other at 7 ppm (labeled as peak 3 in the figure). This agrees well with the results of others (*18–22*). They have been assigned, respectively, to the $AlO_4$ tetrahedral and $AlO_6$ octahedral coordinate sites.

In contrast the $AlPO_4$ (P/Al = 1.0) spectrum has a dominant resonance at 36 ppm (labeled as peak 2 in the figure) and a weaker one at 7 ppm. The dominant peak has been assigned (*20–22*) to the $Al(OP)_4$ tetrahedral environment. The weak resonance at 7 ppm has also been observed by others (*21, 22*) as a weak shoulder. We shall tentatively assign it to $AlO_6$ sites which may occur in the tridymite framework of $AlPO_4$ as a result of lattice disorder. Other $AlO_6$ octrahedral peaks have also been reported at −7 and −21 ppm in hydrated $AlPO_4$ and in certain more highly charged aluminates (*21, 22*). Since our samples had been calcined at 600°C, no evidence for these sites was observed.

In the aluminophosphates the same tetrahedral and octahedral resonances are again observed. The octrahedral peak remains at 7 ppm for each sample but the intensity of the signal decreases as more phosphate is added. At P/Al = 0.2–0.4 one can almost discern a shoulder at −11 ppm, the meaning of which is unclear.

The aluminophosphate tetrahedral peaks are more interesting. They are very broad, compared to $AlPO_4$ and $Al_2O_3$, and are located between these two extremes. As phosphate is added, the tetrahedral intensity increases, and the position of the peak shifts downfield.

### *$^{31}P$ Solid State NMR*

There is only one $^{31}P$ resonance in the $AlPO_4$ and the aluminophosphate spectra. This is shown in Fig. 7. This resonance shifts toward lower field as the P/Al ratio decreases, indicating the $^{31}P$ nucleus is less shielded. The observed shifts in $^{31}P$ NMR imply that there is a gradual change in the electronic environment at the phosphorus sites as the P/Al ratio varies. This reflects a gradual change in the chemical environment around the phosphorus atom. In all these samples, regardless of P/Al ratio, each phosphorus atom has a local $P(OAl)_4$ tetrahedral coordination. The observed $^{31}P$ chemical shift must therefore reflect changes in the electronic environment of the Al atoms. This is consistent with the results in Fig. 6. First, there is a slight shift in the Al tetrahedral resonance in the aluminophosphate before it splits into two resonances at lower P/Al ratio. Also we observed a conversion of the Al tetrahedral sites to the Al octahedral sites as the P/Al ratio is lowered.

### *Ethylene Polymerization*

For ethylene polymerization tests, each aluminophosphate support was impregnated with 1% Cr and calcined at 600°C in dry air, which converted most of the chromium into a hexavalent surface species (*10*). This is thought to occur through a reaction with surface hydroxyls so that each chromium is directly linked to the support, and therefore highly influenced by it.

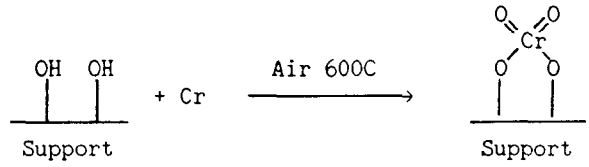


On contact with ethylene in a high pressure reactor, a series of several reactions takes place. The first step is a reduction of $Cr^{6+}$ by ethylene to a lower valent active species, probably $Cr^{2+}$ (*10*). Then the site is alkylated, and ethylene polymerization begins. So the observed activity for polymerization is not just a function of how fast ethylene is incorporated at each site, but also of how many sites have formed during the initial steps. The efficiency of each step is highly dependent on the support.

This is very clear in Fig. 8, which plots the polymerization activity as a function of the P/Al ratio in the support. Although alumina has a high surface area, and stabilized a considerable quantity of hexavalent chromium against thermal decomposition, it results in a very poor polymerization catalyst. This suggests that when the chromium is linked to alumina it is not very efficient for ethylene polymerization. Even prereducing the Cr/alumina catalyst in CO at 300°C does not help very much. So there must be something fundamentally wrong with the alumina environment.

As phosphate is added to the recipe, however, activity improves, as seen in Fig. 8. Two types of hydroxyls have been identified on the surface of $AlPO_4$ (*5*), one attached to aluminum, and the other to phosphate. Therefore it is possible that some of the chromium becomes attached directly to phosphate, and this may be the active form. Certainly these catalysts behave very differently from Cr/silica. The activity peaks, however, at P/Al = 0.8 and thereafter it declines sharply as P/Al approaches unity. This is probably not due to a chemical difference, but to the decreasing surface area and porosity which, as we have seen earlier, accompany the development of $AlPO_4$ crystallinity.

Actually two reactions compete during polymerization on all chromium oxide catalysts. Ethylene can incorporate into the growing chain, or it can serve as a chain transfer agent:

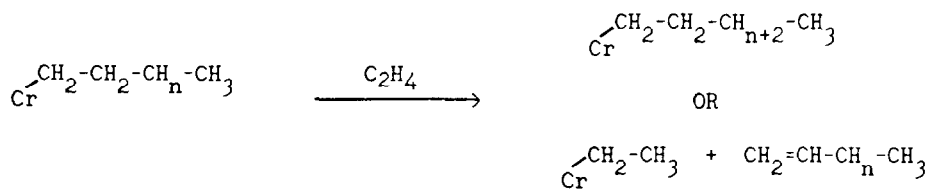


The average polymer chain length produced over each catalyst is a result of these competing reaction, and is thus also stronlgy influenced by the character of the support. This is shown in Fig. 8 by the intrinsic viscosity of these polymers and by the high load melt index (HLMI), which is the measure of the flow of the molten polymer. Decreasing molecular weight (MW) is indicated by lowered viscosity and increasing HLMI.

In Fig. 8 we see that Cr/alumina produces extremely high MW polymer, indicating that the transfer reaction is very sluggish, as is the polymerization itself. As phosphate is added to the support, however, the transfer reaction accelerates, as does the overall polymerization, and shorter chains

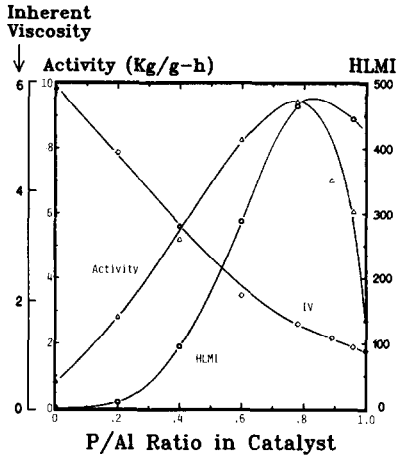


FIG. 8. Porous aluminophosphates were impregnated with 1% Cr and calcined at 600°C to form a polymerization catalyst. On exposure to ethylene each generated polymer at the rate shown. High load melt index (HLMI) and intrinsic viscosity (IV) of the polymer show that the chain transfer rate on each catalyst also depends on the P/Al ratio in the support.

are produced. The more phosphate added, the lower of the MW of the polymer. This may indicate direct attachement of the chromium to phosphate. Unlike the overall polymerization activity, which is influenced by the fragmentation of the support along the larger pores, the transfer rate is much less affected by the porosity of the support. Therefore there is no sharp change in MW as the porosity declines near P/Al = 1.0. Instead the transfer rate may be a more direct reflection of the chemical environment around each active site. If so, it indicates an overwhelming influence by phosphate because the range covered in Fig. 8 is extremely broad in comparison to Cr/silica catalysts.

## DISCUSSION

Two possibilities come to mind when considering the structure of these aluminophosphate precipitates. First, the ingredients could be randomly arranged on a molecular level. That was, after all, the intent when gelation conditions were chosen. Aluminum and phosphate ions were premixed in concentrated solutions, then gelled as quicly as ammonia could be added. But without some consideration of the matter one cannot automatically rule out the second possibility, that these gels are simply intimately mixed domains of alumina and aluminum phosphate.

The thermogravimetric experiments could be construed as evidence for this latter view. Two types of moisture seem to be evolved from each sample, one typical of alumina, the other of $AlPO_4$. But if true, one would expect other properties also to be an average of the two extremes, and this does not seem to be the case.

For example, the porosity of these materials is not at all simple. The surface area is high for alumina, and low for $AlPO_4$. But in between it rises to a maximum at P/Al = 0.2, then there is a plateau at 0.4 to 0.8, and then a sharp decline as P/Al approaches unity. The other porosity measurements are equally nonlinear. The mid-size pores in Fig. 3 show a dramatic change from alumina with the first addition of phosphate.

Neither do the X-ray diffraction patterns support the "two-domains" view. At P/Al = 0 the XRD pattern looks like alumina, and at P/Al= 1.0 it looks like $AlPO_4$. But in between there is no evidence of either crystalline material being present.

One could still argue that the domains of alumina and $AlPO_4$ are too small to be identified by XRD. Fortunately the solid state NMR focuses on the local environment of Al and P nuclei. In Fig. 7 we see that the $^{31}P$ resonance is not constant, as would be expected if the phosphorous atoms were always in an $AlPO_4$ domain. Instead it shifts with P/Al ratio, indicating that the environment of the phosphate is also changing. Since the phosphorous is always tetrahedrally coordinated in all of these materials, as $P(OAl)_4$, this shift must be due to differences in more distant neighbor coordination. For example in $AlPO_4$ the neighboring aluminum atoms are almost entirely $\equiv$P–O–Al$(OP)_3$-type ions, whereas at P/Al = 0.2 they are probably more like $\equiv$P–O–Al$(OAl)_5$. Hence the shifting $^{31}P$ resonance.

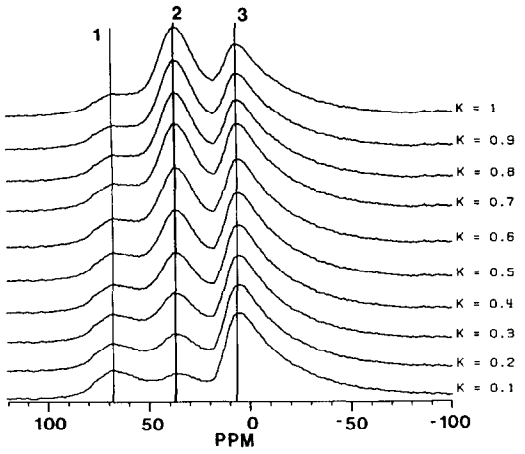


FIG. 9. Linear combinations of the $Al_2O_3$ and $AlPO_4$ spectra in Fig. 6 cannot reproduce the $^{27}Al$ NMR spectra of the intermediate aluminophosphates. This suggests that the aluminophosphates are not simple domains of the two extremes, but instead more complicated species are present. $K = AlPO_4/Al_2O_3$.

The $^{27}Al$ NMR resonance in Fig. 6 leads to a similar conclusion. Although the octahedral peak $AlO_6$ is not very informative (having the same position in both alumina and $AlPO_4$), the tetrahedral peak is far more revealing. There is a considerable chemical shift between $Al(OAl)_4$ in alumina, and $Al(OP)_4$ in aluminum phosphate. Domains in the intermediate samples would produce two resonances corresponding to various combinations of these same two peaks. Instead we see a broad resonance which suggests the presence of several intermediate species, such as $Al(OAl)_n(OP)_{4-n}$.

Furthermore, Fig. 9 shows various linear combinations of the two extreme $^{27}Al$ spectra representing domains of alumina and $AlPO_4$. None of the spectra of the aluminophosphates in Fig. 6 can be reproduced by any of these combinations.

It is, of course, well known (*18, 19*) that in most types of transitional alumina, a good fraction of the aluminum is tetrahedrally coordinated, as $Al(OAl)_4$. The only exceptions are those calcined above 1000°C. In our spectra this resonance occurs at 66 ppm. Notice in Fig. 6, however, that there is only a weak signal at 66 ppm in the P/Al = 0.2 spectrum, even less at P/Al = 0.4, and it almost disappears at P/Al = 0.6. This is consistent with a statistical population of $Al(OAl)_n(OP)_{4-n}$ within the aluminophosphate matrix, and indicates that "free" alumina is not present in these materials. Obviously as the P/Al ratio approaches zero, the support will become more like alumina, and at some point $Al(OAl)_4$ and $Al(OAl)_6$ sites will become abundant. However, even at P/Al = 0.2 we see that the spectrum is still quite unlike that of alumina. This is reasonable since at P/Al = 0.2 each aluminum atom still has roughly one phosphate neighbor.

The results from ethylene polymerization studies in Fig. 8 also seem to agree with this view of the catalyst. Polymerization activity of the aluminophosphate samples is not a simple average of the $AlPO_4$ and $Al_2O_3$ activities. Both alumina and $AlPO_4$ were quite sluggish when promoted with 1% Cr. But the intermediate aluminophosphates exhibited high activity, and a maximum was reached somewhere around P/Al = 0.8–0.6.

It is clear in Fig. 6 that as the P/Al ratio is decreased, tetrahedral sites are converted into octahedral sites. This may be the source of the two types of water detected by TGA. It is very tempting to assign the polymerization activity to these tetrahedral sites. The catalyst precursor, a surface $Cr^{6+}$ species, is tetrahedral, and the only other suitable support is silica, also tetrahedral. This would explain why alumina, a poor support, still has some marginal activity, and why saturating the surface with chromium does not further improve activity. The sharp drop in activity as P/Al approaches unity is almost certainly a result of the decreasing porosity and is not due to any chemical change (*10*). Still, it is hard to know whether the activity really correlates with tetrahedral coordination, or just with the amount of phosphate in the catalyst, since the two go together.

The chain transfer rate, as indicated in Fig. 8 by the HLMI and intrinsic viscosity

of the polymer, does seem to shed much light on the problem. Both functions could be construed as a rough average between the alumina and $AlPO_4$ extremes. But this says nothing about the structure of the support or the coordination, since phosphate is known to enhance the transfer rates on a catalyst (*10*). Thus the more phosphate added, the shorter the chain length. This has nothing to do with tetrahedral coordination since silica, which is already tetrahedral, can also be enhanced by adding phosphate (*24*).

## ACKNOWLEDGMENTS

Many thanks to Dr. Steve Doun at Phillips Research, who obtained the X-ray diffraction patterns in this study. We also gratefully acknowledge the Colorado State University Regional NMR Center, and funding by National Science Foundation Grant CHE-820-8821.

## REFERENCES

1. Kerber, H., and Platz, R., U.S. Patent 2,930,789, March, 1960.
2. Moffat, J. B., Phosphates as catalysts, *Catal. Rev. Sci. Eng.* **18,** No. 2, 199 (1978).
3. Van Wazer, J. R., "Phorphorous and Its Compounds." Wiley–Interscience, New York, 1966.
4. Kearby, K., *in* "Proceedings, International Congress on Catalysis, 2nd (Paris, 1960), p. 2567. Technip, Paris, 1961.
5. Peri, J. B., *Discuss. Faraday Soc.* **52,** 55 (1971).
6. Campelo, J. M., Garcia, A., Gutierrez, J. M., Luna, D., and Marinas, J. M., *Colloids Surf.* **8,** 353 (1984).
7. Gates, B. C., Katzer, J. R., and Schuit, G. C. A., *in* "Chemistry of Catalytic Processes." McGraw–Hill, New York, 1979.
8. McDaniel, M., and Johnson, M. M., U.S. Patent 4,364,842; 4,364,854; and 4,364,855; December, 1982.
9. Bozik, J. E., Vogel, R. F., Kissin, Y. V., and Beach, D. L., *J. Appl. Polym. Sci.*, **29,** 3491 (1984).
10. McDaniel, M. P., *Adv. Catal.* **33,** 47 (1986).
11. Hill, R. W., Kehl, W. L., and Lynch, T. J., U.S. Patent 4,219,444, August, 1980.
12. Marcelin, G. M., Vogel, R. F., and Swift, H. E., *J. Catal.* **83,** 42 (1983).
13. Vogel, R. F., and Marcelin, G., *J. Catal.* **80,** 492 (1983).
14. Schmidtmeyer, A., and Moffat, J. B., *J. Catal.* **96,** 242 (1985).
15. Schmidtmeyer, A., and Moffat, J. B., *Mater. Chem. Phys.* **13,** 409 (1985).
16. Kearby, K. K., U.S. Patent 3,271,299, September, 1966.
17. Pine, L. A., U.S. Patent 3,904,550, October, 1973.
18. Mastikhin, V. M., Krivoruchko, O. P., Zolotovskii, B. P., and Buyanov, R. A., *React. Kinet. Catal. Lett.* **18,** 117 (1981).
19. John, C. S., Alma, N. C. M., and Hays, G. R., *Appl. Catal.* **6,** 341 (1983).
20. Muller, D., Gessner, W., Behrens, H. J., and Scheler, G., *Chem. Phys. Lett.* **79,** 59 (1981).
21. Muller, Von D., Grunze, I., Hallas, E., and Ladwig, G., *Z. Anorg. Allg. Chem.* **500,** 80 (1983).
22. Blackwell, C. S., and Patton, R. L., *J. Phys. Chem.* **88,** 6135 (1984).
23. Rothwell, W. P., Shen, W. X., and Lunsford, J. H., *J. Amer. Chem. Soc.* **106,** 2452 (1984).
24. McDaniel, M. P., and Johnson, M. M., U.S. Patent 4,364,840, December, 1982.